

Article

Effect of Nanobubbles on the Flotation Behavior of Microfine-Grained Serpentine

Bingang Lu^{1,2}, Weiguang Xu^{3,4,5,6,7,*}, Chunhua Luo^{1,2,*}, Wenjuan Li^{3,4,5,6,7}, Xiaohui Su^{1,2}, Yongsheng Song^{3,4,5,6,7}, Jianhang Zhou^{3,4,5,6,7} and Kaiguo Li^{3,4,5,6,7}

- ¹ National Key Laboratory of Ni&Co Associated Minerals Resources Development and Comprehensive Utilization, Jinchang 737100, China; 13830587684@163.com (B.L.); xiaohui8001@163.com (X.S.)
 - ² Jinchuan Nickel & Cobalt Research and Engineering Institute, Jinchang 737100, China
 - ³ National Engineering Research Center for Environment-Friendly Metallurgy in Producing Premium Non-Ferrous Metals, GRINM Group Corporation Limited, Beijing 100088, China; juanzi88888@126.com (W.L.); sysmba@163.com (Y.S.); zhujianhang8888@163.com (J.Z.); likaiguo139@139.com (K.L.)
 - ⁴ GRINM Resources and Environment Tech. Co., Ltd., Beijing 100088, China
 - ⁵ General Research Institute for Nonferrous Metals, Beijing 100088, China
 - ⁶ Beijing Engineering Research Center of Strategic Nonferrous Metals Green Manufacturing Technology, Beijing 100088, China
 - ⁷ GRIMAT Engineering Institute Co., Ltd., Beijing 101407, China
- * Correspondence: xuweiguang@grinm.com (W.X.); china540@163.com (C.L.);
Tel.: +86-10-18713827621 (W.X.); +86-10-15097020780 (C.L.)

Abstract: At present, scholars mainly study the relationship between nanobubbles and useful minerals, often ignoring the influence of bubbles on fine gangue minerals. When selecting nickel sulfide ore, scholars often faced with muddled and irrepressible serpentine, which seriously affects the quality of the concentrate. This muddled serpentine mineral often enters foam products with bubbles. In this study, the role of nanobubbles in the flotation behavior of hydrophilic serpentine was examined. Nanobubbles were successfully prepared via ultrasonic cavitation, with sizes ranging from 50 to 250 nm. The size and number of bubbles produced at 1 min and 2 min of sonication were significantly better than those of the prolonged test group, and it was found that longer sonication time did not produce better results. The stability of the nanobubbles produced via ultrasound was studied, and it was found that the nanobubbles were stable, with no change in size and only a slight decrease in number as the resting time increased. Nanobubbles were introduced into serpentine flotation, we found that the presence of nanobubbles significantly reduced the flotation recovery of serpentine. The presence of nanobubbles reduced the froth entrainment rate of microfine-grained serpentine, which in turn reduced its flotation rate. In the depressant group trials, it was found that the nanobubbles also reduced the amount of depressant. In short, the presence of nanobubbles can prevent the floating of fine hydrophilic gangues during flotation.

Keywords: nanobubbles; serpentine; bubble diameter; recovery; entrainment



Citation: Lu, B.; Xu, W.; Luo, C.; Li, W.; Su, X.; Song, Y.; Zhou, J.; Li, K. Effect of Nanobubbles on the Flotation Behavior of Microfine-Grained Serpentine. *Minerals* **2023**, *13*, 1299. <https://doi.org/10.3390/min13101299>

Academic Editor: Jan Zawala

Received: 14 August 2023

Revised: 20 September 2023

Accepted: 2 October 2023

Published: 7 October 2023



Copyright: © 2023 by the authors. Licensee MDPI, Basel, Switzerland. This article is an open access article distributed under the terms and conditions of the Creative Commons Attribution (CC BY) license (<https://creativecommons.org/licenses/by/4.0/>).

1. Introduction

Froth flotation represents a widely employed technique within the realm of mineral in mineral processing, particularly in the context of sulfide ore separation. It is a physico-chemical process based on assessing the surface chemistry differences in the presence of flotation chemicals between valuable/economical minerals and gangue minerals using bubbles in the pulp. The particle size of minerals is an essential factor affecting flotation efficiency [1]. For the conventional flotation of sulfide ores, the optimal particle size range typically falls within the spectrum of 0.01 to 0.3 mm. Still, with the depletion of high-quality resources, it becomes necessary to process poor ores with extremely fine inlay grain size, which is somewhat overwhelming for conventional flotation techniques. In this regard, numerous studies have found that nanobubble flotation can improve the flotation

of fine-grained minerals [2,3]. Nanobubbles, alternatively referred to as microbubbles, are minute bubbles with diameters measuring less than 1 μm [4]. Various methods have been developed for their production, encompassing techniques such as solution replacement [5], electrochemical electrolysis [6], ultrasonication [7], and hydrodynamic cavitation [8,9]. One of the main reasons for the preparation of nanobubbles using ultrasound is that sound waves cause liquid to fluctuate between negative and positive pressure, where the gas nuclei in the water form and grow during the negative pressure period and then contract during the favorable pressure period. The bubbles burst if they exceed a critical size [10]. Ultrasonic bubble formation occurs away from the pressure wave belly. The resulting bubbles form in filamentous dendritic clusters, which are, in turn, surrounded by many tiny bubbles that repeatedly clump together and break up [11]. Under the action of cavitation and primary Bjerknes forces in the ultrasonic field, the gas nuclei on the particle surface gradually grow, aggregate, and then form tiny bubbles, driving the particles to aggregate at the acoustic pressure nodes [12]. In a study by Chen et al. [13], it was observed that, under 200 kHz high-intensity focused ultrasound (HIFU), only stable cavitation bubbles were generated on the hydrophobic silica surface. This in turn contributed to particle agglomeration, while no accumulation was formed in the hydrophilic silica suspension.

With the in-depth study of nanobubbles, many research results have shown [14–17] that nanobubbles with large specific surface area and high surface energy are more selective than general bubbles and easily attach to hydrophobic solid surfaces [13,18]. When nanobubbles approach proximity, they establish nanobubble bridges [19], a phenomenon that fosters the agglomeration of microfine mineral particles, bolstering the flotation uplift process. Chen et al. [20] harnessed ultrasonic standing waves operating at 200 kHz to treat finely grained coal, inducing cavitation bubbles to form on the surfaces of hydrophobic coal particles. If the size of the cavitation bubble is larger than the resonance radius, bubble-filled coal particles move to the nodes of the ultrasonic standing wave due to an acoustic radiation force, leading to the rapid aggregation of fine coal particles. Micro-flotation results show that flotation efficiency is significantly improved after ultrasonic standing wave treatment.

Mitra et al. [21] undertook an investigation involving a suspension of hydrophobic glass microspheres characterized by larger particle sizes, employing periodic ultrasonic pulses to do so. The ultrasonic pulses caused the creation of many cavitation bubbles in the liquid in the acceptable size range. It was observed that these bubbles formed particle clusters with the glass microspheres, which attached to relatively large carrier bubbles to form stable bubble–particle aggregates that subsequently floated upwards. Fan et al. [22] found that nanobubbles significantly reduced the bubble rise rate, increasing the air inclusion rate and improving coarse-grained phosphate froth flotation. The presence of nanobubbles in the flotation pulp reduced the rinsing velocity of conventional particle-size bubbles, prolonged the bubble–particle sliding time (contact time), and reduced the tangential sliding velocity of particles on the bubble surface, thereby increasing the probability of bubble–particle attachment and decreasing the probability of detachment. Ahmadi et al. [23] delved into an investigation regarding the influence of nanobubbles on the flotation recovery of microfine- and ultrafine-grained chalcopyrite. Their findings demonstrated that the presence of nanobubbles substantially augmented the recovery rates of chalcopyrite fines and ultra-fines by an impressive margin ranging from 16% to 21%. Furthermore, the incorporation of nanobubbles led to remarkable reductions in the dosages of both the trapping agent (by 75%) and the frothing agent (by 50%).

Sobhy and colleagues [24] conducted a study involving the implementation of nanobubble column flotation for coal processing. They improved the flotation recovery of fine-grained coal by 5 to 50% depending on the process operating conditions, and the amount of frother was reduced by 1/3. Tao [25] investigated the use of nanobubbles for the anionic reverse flotation of hematite and found that their effects significantly improved the grade and recovery of the concentrate. Sobhy [26] calculated that the application of nanobubbles increased the kinetic flotation rate constant by 41%, which implied a significant increase

in processing capacity. The nanobubbles encapsulated particles and formed aggregates, thus increasing the probability of particle bubble collisions. Furthermore, the induction time of nanobubbles generated on the surface of hydrophobic particles was reduced by 1/2, thereby increasing the attachment probability.

Liao et al. [27] found that micro- and nanobubbles could enhance the flotation of fine-grained monohydrate hard alumina minerals and significantly improve the flotation recovery of fine-grained monohydrate hard alumina. Taghavi et al. [28] found that nanobubbles significantly improved the flotation recovery of pure magnesite. Lei [29] investigated the role of nanobubbles in the coal–kaolin system, finding that nanobubbles can affect the aggregation state and the degree of kaolinite coverage on the surface of coal particles. On the one hand, nanobubbles fostered the formation of kaolin aggregates. Conversely, the presence of a nanobubble layer hindered the coverage of coal particle surfaces by kaolin, leading to the aggregation of kaolin particles on the surface of coal particles with limited coverage.

Etchepare et al. [30] investigated the flotation effect of nanobubbles on hydrophilic $\text{Fe}(\text{OH})_3$ colloidal precipitates. Due to the higher lifting force of microbubbles, the flotation rate was faster. Still, the separation effect was inferior to that of nanobubbles, and so nanobubbles were used in combination with microbubbles to solve the problem of slow flotation rate when using nanobubbles alone. They attributed the increased recovery of hydrophilic $\text{Fe}(\text{OH})_3$ precipitates to the entrapment of micro/nanobubbles inside the flocs and solid entrainment by water. Zhou et al. [31] used AFM to find that nanobubbles are difficult to nucleate on highly hydrophilic white mica surfaces and can form stably on sufficiently hydrophobic mineral surfaces. Once nanobubbles are stably nucleated on hydrophobic mineral surfaces, the attraction between mineral particles is greatly enhanced, thus promoting the aggregation and flotation of fine-grained minerals. At the same time, due to the high selectivity of nucleation of nanobubbles on solids, high separation efficiency can also be obtained in separating hydrophobic target minerals from hydrophilic polymeric minerals. Therefore, increasing the temperature during slurry conditioning may be a potential way to improve the flotation performance of minerals. Tsave et al. [32] discovered that the adherence of microbubbles to the surfaces of fine particles facilitated the attachment of standard-sized bubbles, ultimately improving the flotation recovery of these particles. Zhang et al. [33] noted that nanobubbles reduced the amount of trapping agent used, made flotation faster, and led to particles exhibiting significant aggregation behavior and high adhesion probability.

Researchers have made significant strides in leveraging nanobubbles to enhance the recovery of minerals at the microfine particle size [23,24]. However, vein minerals are not negligible in size, while valuable minerals are finely ground. In particular, for quickly muddied magnesium silicate hydrates, many flotation conditions have not reached the delicate grinding process, which still produces many microfine-grain veinlets, seriously affecting the recovery of valuable minerals. Therefore, in this study, the properties of nanobubbles generated via ultrasonication were investigated by preparing nanobubbles and testing the bubbles' stability. And the flotation behavior of serpentine was investigated by combining nanobubbles with large bubbles of the flotation machine. In the flotation of nickel sulfide ore, easily muddied serpentine minerals have a great impact on the flotation process. Therefore, nanobubbles were prepared via the ultrasonic method and their stability was detected to explore the properties of nanobubbles generated by ultrasound. The nanobubbles were then combined with larger bubbles, typically generated by flotation machines, to scrutinize their impact on the flotation behavior of hydrophilic serpentine. The aim was to examine the influence of nanobubbles on the flotation behavior of hydrophilic serpentine and to reveal their role in optimizing the flotation mechanism of microfine-grained refractory ores.

2. Materials and Methods

2.1. Materials

Serpentine, chemical formula $Mg_6[Si_4O_{10}](OH)_8$, is often divided into three types: lizardite, antigorite, and chrysotile. The serpentine ore used in this study was taken from the Xiuyan jade mine in Liaoning Province, China, and the results of X-ray diffraction (XRD) analysis are shown in Figure 1. Analysis of the sample was conducted using a D/Max-III A X-ray diffractometer (Malvern Panalytical, Shanghai, China) with Cu $K\alpha$ radiation at 40 kV and 30 mA and with a scanning rate of 15 ($^\circ$)/min from 5 $^\circ$ to 70 $^\circ$.

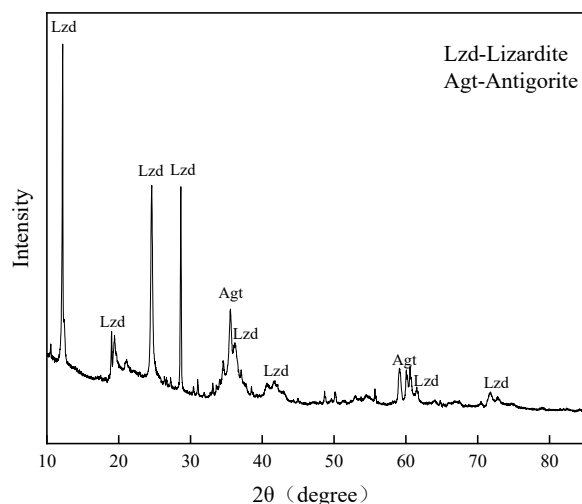


Figure 1. XRD diffraction pattern of serpentine.

Figure 1 shows that the main components of this serpentine ore are lizardite and antigorite minerals. The samples were sent for chemical multi-element analysis. The minerals were uniformly represented and dissolved samples for ICP detection (ICP-OES, Agilent Technologies Inc., Agilent 700, In Santa Clara, CA, USA). The results are shown in Table 1. The data calculation in the table indicates that the purity of serpentine was found to exceed 96%, thus reaching the level required for pure mineral experiments.

Table 1. Serpentine chemical multi-element analysis results.

| Elements | Mg | Si | Al | Cl | Fe | S | Ca |
|-------------|-------|-------|------|------|------|------|------|
| Content (%) | 33.94 | 24.88 | 0.49 | 0.37 | 0.32 | 0.25 | 0.16 |

2.2. Methods

2.2.1. Preparation of Nanobubbles

Nanobubbles were generated by utilizing the LC-1500 ultrasonic crusher, manufactured by Shanghai Bingyue Electronic Instrument Co., Ltd. (Shanghai, China). The detection and characterization of nanobubbles were performed using a BeNano 90 nanoparticle size analyzer, a product by Bettersize Instruments (Dandong, China), which is capable of measuring particles within a size range spanning from 2 nm to 36 μ m. The measurement error was less than 1%. Measurement was carried out at 22 $^\circ$ C, with 15 mL of the cavitated solution used for detection. The process was repeated three times for each group of specimens to obtain six measurements. Additionally, the viscosity of the pulp following ultrasonication was assessed using a viscometer, specifically the SNB-2 model from Shanghai Jingtian Electronic Instrument Co., Ltd. (Shanghai, China), which features a wide measuring range of 1 to 6,000,000 mPa·s, allowing for comprehensive viscosity analysis.

2.2.2. Nanobubble Flotation Experiments

The agents used were sodium hydroxide (purchased from Shanghai Macklin Biochemical Technology Co., Ltd., Shanghai, China); AR 95%, used as a pH adjuster; Sodium O-butyldithiocarbonate (obtained from Beijing Chemical Industry Group Co., Ltd., Beijing, China); AR 95%, used as a collector; pine alcohol oil (also sourced from Beijing Chemical Industry Group Co., Ltd., Beijing, China); AR 95%, used as a frother; and sodium carboxymethyl cellulose (CMC), used as a depressant (supplied by Shanghai Macklin Biochemical Technology Co., Ltd., Shanghai, China). The ore samples used in the flotation experiments were subjected to crushing, grinding, and sieving processes, yielding five distinct particle-size fractions: 45–74 μm , 38–45 μm , 30–38 μm , 15–30 μm , and <15 μm .

Since a lot of research has been conducted using ultrasonic pretreatment slurry flotation, we know that the main effects are the cavitation effect and the acoustic radiation force effect. The cavitation effect causes the precipitation of dissolved gases in the liquid to form bubbles. Conversely, the acoustic radiation force effect is observed in flotation through actions such as mineral sludge package removal, oxide film detachment, and agent dispersion [20,21]. The objective of this experiment was to investigate the interactions between micro- and nanobubbles and mineral flotation. For this purpose, the experimental procedure involved subjecting 20 mL of a 100 mL pure water sample to ultrasonic treatment via the LC-1500 ultrasonic crusher, employing fixed-duration ultrasound, as depicted in Figure 2.

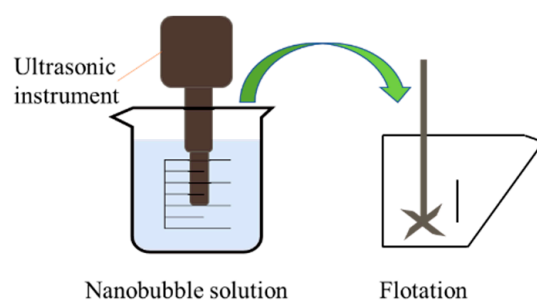


Figure 2. Schematic diagram of micro- and nanobubble flotation.

The flotation experiments were carried out in an XFG-type hanging tank flotation machine (manufactured by Jilin Exploration Machinery Plant, Changchun, China, XFGII5). We took 2.0 g of sample each time, and added 20 mL of pure water (sourced from PINE-TREE XYF2-40-H, Beijing Xianshunyuan Technology Co., Ltd., Beijing, China) after sonication; we then adjusted the pH to 10 using NaOH, and stirred for 3 min. Next, 15 mg/L of sodium O-butyldithiocarbonate and 1×10^{-4} mol/L of pine alcohol oil were added as a collector and frother, respectively, and the flotation was carried out for 3 min. The float and sink products were collected, dried, and weighed, and the flotation recovery was calculated. The flotation machine speed was 1600 r/min.

3. Results and Discussion

3.1. Nanobubble Generation via Ultrasonication

To explore the most favorable conditions for the generation of micro- and nanobubbles through sonication, a series of experiments were conducted involving the sonication of pure water for varying durations: 1 min, 2 min, 5 min, and 10 min, with a control group maintained at 0 min of sonication. These experiments were carried out at a temperature of 25 °C. Each experimental group underwent three repetitions, and the outcomes are graphically depicted in Figure 3. Furthermore, the influence of different ultrasonic durations on the stability of the slurry and its viscosity was investigated, with the results presented in Figure 4.

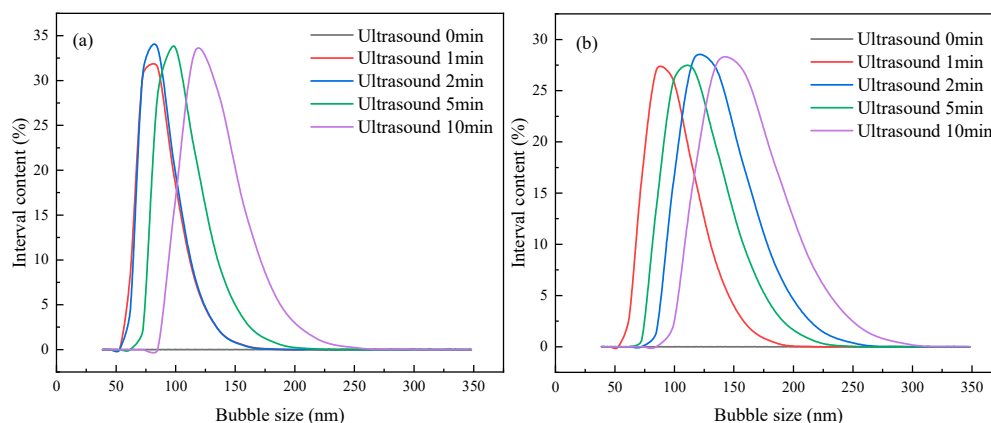


Figure 3. Effect of ultrasonic time on the size distribution of nanobubbles. (a) Number distribution; (b) volume distribution.

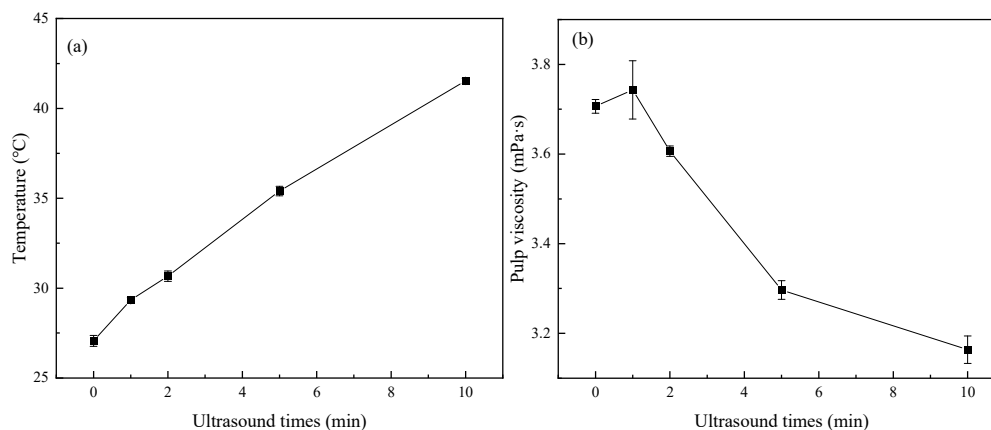


Figure 4. Effect of ultrasonic time on the (a) temperature; (b) pulp viscosity.

Figure 3a illustrates the presence of numerous nanobubbles within the solution subsequent to sonication, with their diameters falling within the range of approximately 50 to 250 nm. As the sonication duration increased, the size of the bubbles increased, and the size of the nanobubbles produced by 1 min and 2 min of sonication was the smallest. Most of the bubbles were about 80 nm in size. The bubbles produced by 5 min of sonication were about 100 nm, while the bubbles generated following 10 min of sonication were approximately 120 nm in size. Figure 3b provides insights into the volume content distribution of bubbles generated at different sonication durations. Figure 3b also shows that the volume contents of bubbles produced by 1 min, 2 min, 5 min, and 10 min of sonication are similar in size and are all about 27%. In contrast, the bubbles produced via 1 min sonication have the smallest size. The smaller the measurements taken when the volumes are the same, the larger the number of bubbles will be. As such, the bubbles produced via 1 min of sonication have the smallest size and are most numerous [34]. Figure 4a shows that, as ultrasonic time increased, the temperature of the slurry gradually rose too. The results in Figure 4b show that, as ultrasonic time increased, the viscosity of the slurry showed a downward trend. The increasing sonication time raised the water temperature, thereby presenting a higher probability of bubble coalescence and leading to larger sizes and volumes of nanobubbles.

The stability of nanobubbles was investigated, and the nanobubble-containing solutions produced via sonication were left for 0 min, 20 min, 40 min, and 60 min after 1 min of sonication. Then, the bubble sizes were measured, and the results are shown in Figure 5.

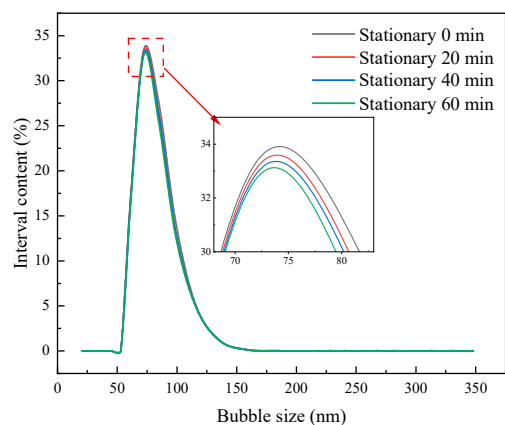


Figure 5. Stability curves of bubbles produced by ultrasonication for 1 min.

The bubble stability curve clearly illustrates that the size of nanobubble generated through ultrasound did not change much with the increasing time. The overall content was stable, which indicated that the nanobubbles were more durable. The produced nanobubbles did not rupture as quickly as conventional bubbles, and some researchers found that most of the nanobubbles present in the solution still existed stably after three months [35].

3.2. Nanobubble Flotation Experiments

The nanobubble flotation experiments were performed by introducing the nanobubble solution generated using ultrasound into the flotation machine. To investigate the impact of the flotation machine on nanobubbles produced through ultrasonic treatment, the distribution of bubbles in water samples was measured 1 min after ultrasonication, at the same time, the gas distribution of the ultrasonic water sample after 9 min of stirring by the flotation machine was measured. It can be seen from Figure 6 that the nanobubbles generated following ultrasonication fell within the size range of approximately 50–150 nm. Additionally, subsequent to agitation in the flotation machine, their size increased to approximately 75–200 nm. Mechanical agitation also caused the aggregation of small-sized bubbles. The bubbles are still within the nanometer size, so the effect of the flotation machine on the flotation of nanobubbles is small. In mechanical flotation, strong agitation could also generate nanobubbles by hydrodynamic cavitation. Therefore, nanobubbles generated via ultrasound and hydrodynamic cavitation co-exist in the system.

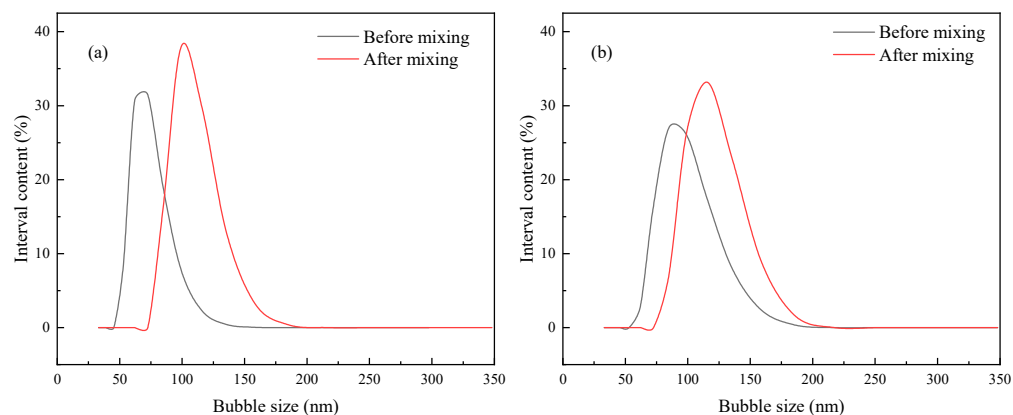


Figure 6. Effect of flotation machine agitation on nanobubbles. (a) Number distribution; (b) Volume distribution.

In order to explore the influence of nanobubbles on serpentine’s flotation behavior, the serpentine recovery rate after ultrasonic pretreatment of the aqueous solution was studied

using nanobubbles generated via ultrasonic cavitation combined with large bubbles generated using the hanging tank flotation machine. The flotation conditions were as follows: pH = 9.5, sodium O-butyldithiocarbonate 15 mg/L, pine alcohol oil 1×10^{-4} mol/L. In the experimental procedure, each set of ultrasonicated solution was allowed to equilibrate to the same temperature it was at before ultrasonication prior to proceeding with the flotation test. This temperature equilibration ensured consistency in the experimental conditions.

As can be seen from Figure 7, the flotation recovery of serpentine increases as its particle size decreases, reaching 25% for $-15 \mu\text{m}$. This trend can be attributed to the increase in the apparent viscosity of the pulp as mineral size decreases, leading to a higher entrainment rate [36]. Although serpentine is a hydrophilic mineral, its slow flotation kinetics, non-selective mucus coverage, and entrainment are carried into the froth layer because the particle size is too small. Ultrasonic treatment can significantly impair the recovery of serpentine, especially for the fine-grained grade. The recovery of serpentine increased slowly with the rise in sonication time. The recovery of serpentine in flotation was lowest after 1 min of sonication because of the small size and large number of bubbles produced during 1 min of sonication. The particle size of microfine-grained serpentine is much larger than that of nanobubbles, and as a hydrophilic mineral it cannot enter nanobubble aggregates, which reduces the entrainment of fine-grained serpentine and thus its recovery. Ultrasound raised the temperature and, in turn, reduced the viscosity of the slurry, thereby reducing the entrainment of fine particles to a certain extent. As Figure 7 shows, the floating amount of serpentine was greater with 10 min ultrasonic than that of the ultrasonic 1 min test group; likewise, the viscosity of slurry was significantly lower with 10 min of ultrasound than with 1 min. These findings indicate that the nanobubbles generated by ultrasound played a major role in reducing the entrainment effect.

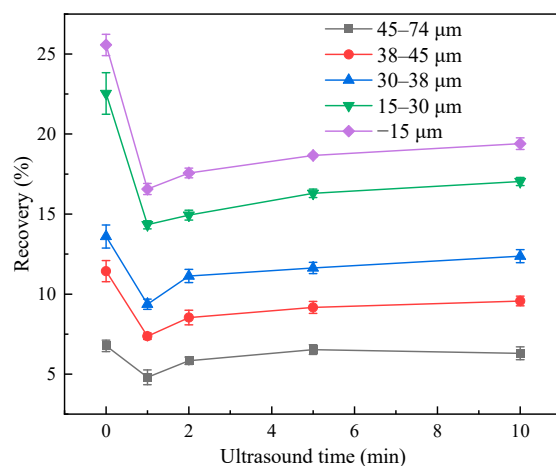


Figure 7. Effect of ultrasonic time on serpentine recovery.

Examination of nanobubble distribution in the concentrate and tailing supernatant after flotation revealed some significant findings, as depicted in Figure 8. In the concentrate, the bubble size ranged from 400 to 1200 nm, while in the tailing it fell within the range of 200 to 500 nm. Notably, these results showed a substantial increase in overall bubble size compared to Figure 5, the results for which were observed after the agitation within the flotation machine. This increase in bubble size suggests that introducing minerals into the system exacerbated the aggregation effect of smaller-sized nanobubbles. It is worth highlighting that the bubble size was substantially larger in the concentrate, and that larger nanobubbles possess enhanced lifting capabilities, making them more likely to rise and become part of the concentrate [30].

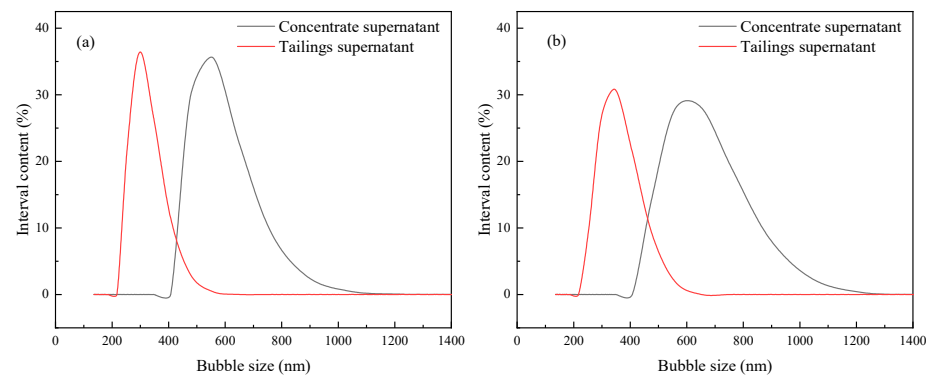


Figure 8. Distribution of nanobubbles in flotation concentrate and tailing. (a) Number distribution; (b) volume distribution.

Next, nanobubbles were introduced, while depressant CMC was added to the system. Figure 9 illustrates that the presence of nanobubbles lowered the recovery of serpentine across all five particle sizes, with the most significant impact observed for 15–30 μm and –15 μm serpentine fractions. A group with nanobubbles present had a lower recovery with the same amount of added depressant. It has previously been reported that the presence of nanobubbles reduces the amount of depressant required [33]. Consistent with that earlier finding, the recovery level of <15 μm serpentine at a depressant concentration of 40 mg/L was equivalent to the recovery of serpentine at a depressant concentration of 25 mg/L in the presence of nanobubbles. This suggests that nanobubbles can effectively reduce the amount of depressant required to achieve the desired level of serpentine recovery, particularly for fine-grained serpentine fractions.

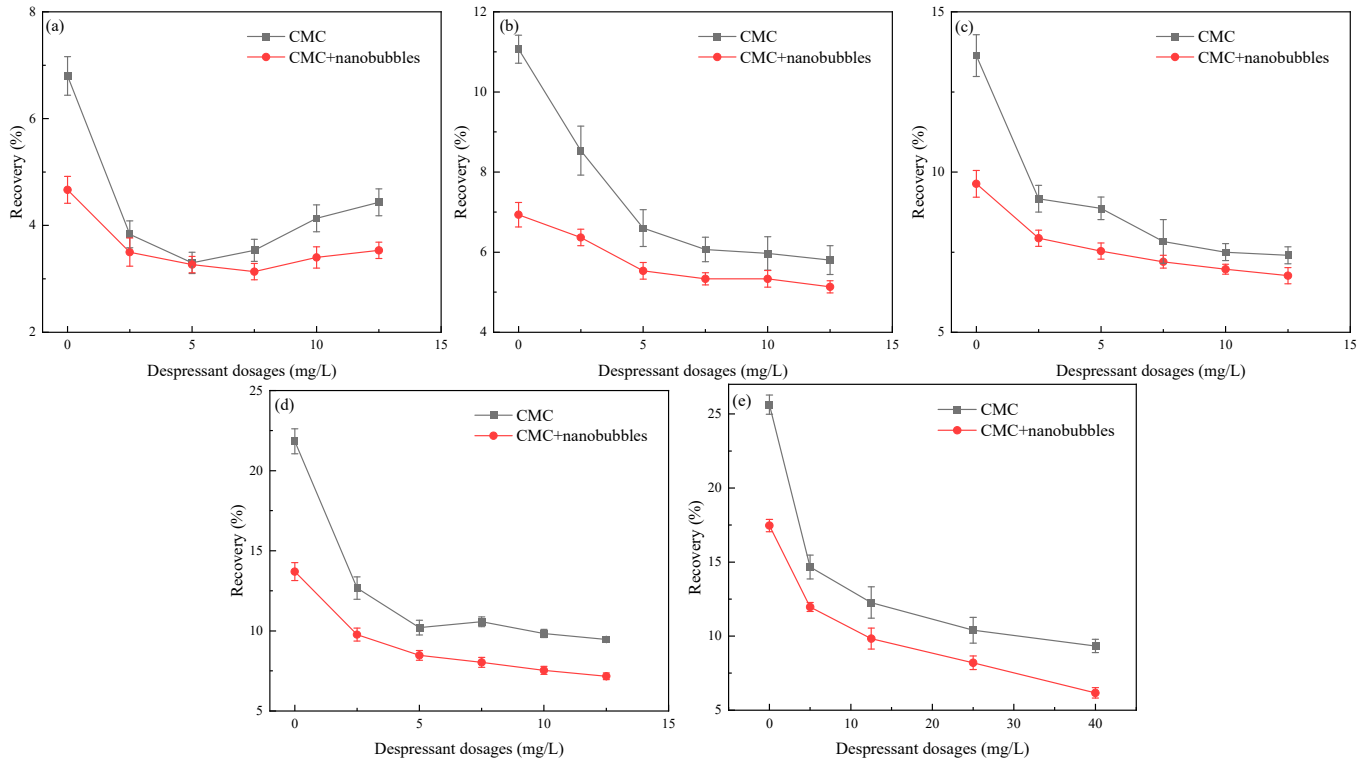


Figure 9. Effect of CMC dosage on the recovery of serpentine in the presence of nanobubbles (pH = 9.5, Sodium O-butyldithiocarbonate 15 mg/L, pine alcohol oil dosage 1×10^{-4} mol/L). (a) 45–74 μm ; (b) 38–45 μm ; (c) 30–38 μm ; (d) 15–30 μm ; (e) –15 μm .

3.3. Analysis of the Mechanism of Nanobubbles to Reduce the Recovery Rate of Microfine-Grained Serpentine

The experimental findings clearly indicate that the presence of nanobubbles reduces the flotation recovery of microfine-grained serpentine. This outcome can be explained by two primary factors. First, the primary mechanisms governing flotation of hydrophilic microfine-grained minerals involve foam entrainment and attachment to the surface of valuable minerals [37]. Given that nanobubbles are significantly smaller than mineral particles, they hinder the adhesion of hydrophilic minerals to valuable mineral surfaces when coming into contact with them [29]. In essence, the presence of nanobubbles disrupts the attachment process, reducing the recovery of hydrophilic serpentine. Second, while the ultrasound-induced reduction in slurry viscosity does contribute to lowering the floatability of hydrophilic serpentine, the dominant factor influencing serpentine flotation is the presence of nanobubbles generated using ultrasound. These nanobubbles play a central role in limiting the attachment and adhesion of serpentine to valuable mineral surfaces, thereby reducing its overall flotation recovery.

Entrainment can be conceptualized as a two-step process involving the movement of particles from the upper pulp to the bubble and then from the bubble to the concentrate. Entrainment is inevitable for both hydrophobic and hydrophilic minerals and is one of the critical factors affecting the concentrate grade [37]. It is important to note that nanobubbles possess relatively weak flotation capabilities; when nanobubbles alone are present, they do not achieve effective mineral recovery [21,30]. In contrast, conventional-sized bubbles exert more significant lifting forces and facilitate faster flotation, as illustrated in Figure 10. During the flotation process, a portion of nanobubbles attaches to the surface of conventional-size bubbles to float, and the domain will exist in the water layer between large bubbles. In addition, the actual volume of nanobubbles produced under natural conditions is very small (gas/bubble holdup $\ll 1\%$ of water), and therefore their effect on water entrainment is negligible. When a large number of nanobubbles exist in the water layer between two large-sized bubbles, that layer has a stronger hydrophobic force on fine-grained hydrophilic minerals; the resulting exclusion of these minerals from the water layer also effectively reduces the entrainment effect.

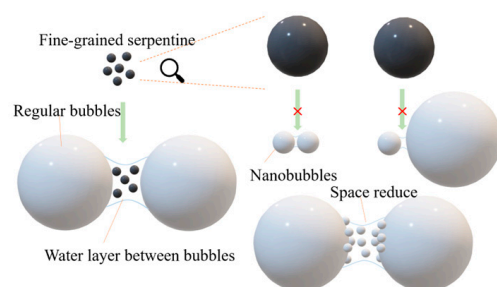


Figure 10. Schematic diagram of nanobubbles reducing the entrainment effect of microfine-grained serpentine.

4. Conclusions

This study investigated the flotation behavior of nanobubbles on the microfine-grained, easily slimed mineral serpentine and yielded the following conclusions:

- (1) Nanobubbles were successfully generated through sonication, and we found that the bubble sizes produced via sonication for 1 min and 2 min were the smallest. The stability of the nanobubbles produced by ultrasonication was also studied, and it was found that the nanobubbles were stable. Their size remained consistent, and only a slight decrease in their number was observed with increasing resting time.
- (2) Single-mineral flotation experiments were conducted on serpentine using nanobubbles generated through sonication, and we found that the presence of nanobubbles significantly reduced the recovery of serpentine, and that the lowest recovery of

serpentine was obtained by sonication for 1 min. The reduction in serpentine flotation recovery in the presence of nanobubbles was mainly due to a decrease in the froth entrainment rate of serpentine at the microfine-grain level.

- (3) Nanobubbles also reduced the amount of depressant required. With the addition of depressant under conditions of 1 min sonication, the recovery level of serpentine in the group without sonication but with 40 mg/L of depressant was equivalent to that of serpentine in the sonicated group, which required only 25 mg/L of depressant to achieve a similar recovery level.

These findings underscore the potential of nanobubbles in mineral flotation processes, particularly for microfine-grained minerals like serpentine, where they can reduce recovery, depressant usage, and froth entrainment.

Author Contributions: Conceptualization, W.X., W.L. and B.L.; methodology, W.X., W.L. and C.L.; validation, W.X., W.L., J.Z. and K.L.; formal analysis, W.X. and Y.S.; investigation, W.X. and C.L.; writing—original draft preparation, W.X. and B.L.; writing—review and editing, W.L. and Y.S.; visualization, B.L. and W.X.; supervision, W.L. and X.S.; project administration, W.L., B.L. and C.L. All authors have read and agreed to the published version of the manuscript.

Funding: This work was financially supported by the National Key Research and Development Project (No. 2022YFC2904202), and the Enterprise entrusted research on Microbubble Flotation Technology of Low-Grade Ore.

Data Availability Statement: Not applicable.

Conflicts of Interest: The authors declare no conflict of interest.

References

- Feng, D.; Aldrich, C. Effect of particle size on flotation performance of complex sulphide ores. *Miner. Eng.* **1999**, *12*, 721–731. [[CrossRef](#)]
- Ma, Y.; Tao, D.; Tao, Y.; Liu, S. An innovative flake graphite upgrading process based on HPGR, stirred grinding mill, and nanobubble column flotation. *Int. J. Min. Sci. Technol.* **2021**, *31*, 1063–1074. [[CrossRef](#)]
- Zhou, W.; Ou, L.; Shi, Q.; Feng, Q.; Chen, H. Different flotation performance of ultrafine scheelite under two hydrodynamic cavitation modes. *Minerals* **2018**, *8*, 264. [[CrossRef](#)]
- Tao, D. Recent advances in fundamentals and applications of nanobubble enhanced froth flotation: A review. *Miner. Eng.* **2022**, *183*, 107554. [[CrossRef](#)]
- Liu, M.; Zhao, W.; Wang, S.; Guo, W.; Tang, Y.; Dong, Y. Study on nanobubble generation: Saline solution/water exchange method. *ChemPhysChem* **2013**, *14*, 2589–2593. [[CrossRef](#)]
- Guan, M.; Guo, W.; Tang, Y.; Hu, J.; Dong, Y. Investigation on the temperature difference method for producing nanobubbles and their physical properties. *ChemPhysChem* **2012**, *13*, 2115–2118. [[CrossRef](#)] [[PubMed](#)]
- Cho, S.H.; Kim, J.Y.; Chun, J.H.; Kim, J.D. Ultrasonic formation of nanobubbles and their zeta-potentials in aqueous electrolyte and surfactant solutions. *Colloids Surf. A Physicochem. Eng. Asp.* **2005**, *269*, 28–34. [[CrossRef](#)]
- Nirmalkar, N.; Patek, A.W.; Barigou, M. On the existence and stability of bulk nanobubbles. *Langmuir* **2018**, *34*, 10964–10973. [[CrossRef](#)]
- Etchepare, R.; Oliveira, H.; Nicknig, M.; Azevedo, A.; Rubio, J. Nanobubbles: Generation using a multiphase pump, properties and features in flotation. *Miner. Eng.* **2017**, *112*, 19–26. [[CrossRef](#)]
- Suslick, K.S.; Doktycz, S.J.; Flint, E.B. On the origin of sonoluminescence and sonochemistry. *Ultrasonics* **1990**, *28*, 280–290. [[CrossRef](#)] [[PubMed](#)]
- Hatanaka, S.; Yasui, K.; Kozuka, T.; Tuziuti, T.; Mitome, H. Influence of bubble clustering on multibubble sonoluminescence. *Ultrasonics* **2002**, *40*, 655–660. [[CrossRef](#)] [[PubMed](#)]
- Chen, Y.; Ni, C.; Xie, G.; Liu, Q. Toward efficient interactions of bubbles and coal particles induced by stable cavitation bubbles under 600 kHz ultrasonic standing waves. *Ultrason. Sonochem.* **2020**, *64*, 105003. [[CrossRef](#)]
- Chen, Y.; Zheng, H.; Truong, V.N.T.; Xie, G.; Liu, Q. Selective aggregation by ultrasonic standing waves through gas nuclei on the particle surface. *Ultrason. Sonochem.* **2020**, *63*, 104924. [[CrossRef](#)] [[PubMed](#)]
- Nazari, S.; Shafaei, S.Z.; Gharabaghi, M.; Ahmadi, R.; Shahbazi, B.; Fan, M. Effects of nanobubble and hydrodynamic parameters on coarse quartz flotation. *Int. J. Min. Sci. Technol.* **2019**, *29*, 289–295. [[CrossRef](#)]
- Ding, S.; Xing, Y.; Zheng, X.; Zhang, Y.; Cao, Y.; Gui, X. New insights into the role of surface nanobubbles in bubble-particle detachment. *Langmuir* **2020**, *36*, 4339–4346. [[CrossRef](#)] [[PubMed](#)]
- Cui, R. Study on the Improvement of Low-Rank Coal and Its Semi-Coke Adsorption on Congo Red Dye by Micro-Nano Bubbles. Master's Thesis, China University of Mining and Technology, Xuzhou, China, 2020.

17. Ma, F.; Zhang, P.; Tao, D. Surface nanobubble characterization and its enhancement mechanisms for fine-particle flotation: A review. *Int. J. Miner. Metall. Mater.* **2022**, *29*, 727–738. [[CrossRef](#)]
18. Azevedo, A.; Etchepare, R.; Calgaroto, S.; Rubio, J. Aqueous dispersions of nanobubbles: Generation, properties and features. *Miner. Engr.* **2016**, *94*, 29–37. [[CrossRef](#)]
19. Hampton, M.A.; Nguyen, A.V. Nanobubbles and the nano-bubble bridging capillary force. *Adv. Colloid Interface Sci.* **2010**, *154*, 30–55. [[CrossRef](#)]
20. Chen, Y.; Xie, G.; Chang, J.; Grundy, J.; Liu, Q. A study of coal aggregation by standing-wave ultrasound. *Fuel* **2019**, *248*, 38–46. [[CrossRef](#)]
21. Mitra, S.; Hoque, M.M.; Evans, G.; Nguyen, A.V. Direct visualisation of bubble-particle interactions in presence of cavitation bubbles in an ultrasonic flotation cell. *Miner. Eng.* **2021**, *174*, 107258. [[CrossRef](#)]
22. Fan, M.; Tao, D.; Rick, H.; Luo, Z. Nanobubble generation and its applications in froth flotation (part II): Fundamental study and theoretical analysis. *Min. Sci. Technol. Chin.* **2010**, *20*, 159–177. [[CrossRef](#)]
23. Ahmadi, R.; Khodadadi, D.A.; Abdollahy, M.; Fan, M. Nano-microbubble flotation of fine and ultrafine chalcopyrite particles. *Int. J. Min. Sci. Technol.* **2014**, *24*, 559–566. [[CrossRef](#)]
24. Sobhy, A.; Tao, D. Nanobubble column flotation of fine coal particles and associated fundamentals. *Int. J. Miner. Process* **2013**, *124*, 109–116. [[CrossRef](#)]
25. Tao, D.; Wu, Z.; Sobhy, A. Investigation of nanobubble enhanced reverse anionic flotation of hematite and associated mechanisms. *Powder Technol.* **2021**, *379*, 12–25. [[CrossRef](#)]
26. Sobhy, A. Cavitation Nanobubble Enhanced Flotation Process for More Efficient Coal Recovery. Master's Thesis, University of Kentucky, Lexington, KY, USA, 2013.
27. Liao, S.; Ou, M.; Zhou, W. Micro-nano bubbles properties induced by hydrodynamic cavitation and their influences on fine mineral flotation. *Chin. J. Nonferrous. Met.* **2019**, *29*, 1567–1574.
28. Tsave, P.K.; Kostoglou, M.; Karapantsios, T.D.; Lazaridis, N.K. A Hybrid Device for Enhancing Flotation of Fine Particles by Combining Micro-Bubbles with Conventional Bubbles. *Minerals* **2021**, *11*, 561. [[CrossRef](#)]
29. Lei, W. Study on the Preparation of Nano-Bubbles and Their Effect on Coal Slime Flotation. Master's Thesis, Wuhan University of Science and Technology, Wuhan, China, 2020.
30. Etchepare, R.; Azevedo, A.; Calgaroto, S.; Rubio, J. Removal of ferric hydroxide by flotation with micro and nanobubbles. *Sep. Purif. Technol.* **2017**, *184*, 347–353. [[CrossRef](#)]
31. Zhou, W.; Wu, C.; Lv, H.; Zhao, B.; Liu, K.; Ou, L. Nanobubbles heterogeneous nucleation induced by temperature rise and its influence on minerals flotation. *Appl. Surf. Sci.* **2020**, *508*, 145282. [[CrossRef](#)]
32. Taghavi, F.; Noaparast, M.; Pourkarimi, Z.; Nakhaei, F. Comparison of mechanical and column flotation performances on re-recovery of phosphate slimes in presence of nano-microbubbles. *J. Cent. South Univ.* **2022**, *29*, 102–115. [[CrossRef](#)]
33. Zhang, Z.; Ren, L.; Zhang, Y. Role of nanobubbles in the flotation of fine rutile particles. *Miner. Eng.* **2021**, *172*, 107140. [[CrossRef](#)]
34. Mo, C. Research on the Generation Method and Properties of Nanobubble Based on Ultrasonic Cavitation. Master's Thesis, University of Chinese Academy of Sciences (Shanghai Institute of Applied Physics, Chinese Academy of Science), Shanghai, China, 2019.
35. Nirmalkar, N.; Pacek, A.W.; Barigou, M. Bulk nanobubbles from acoustically cavitating aqueous organic solvent mixtures. *Langmuir* **2019**, *35*, 2188–2195. [[CrossRef](#)] [[PubMed](#)]
36. Zou, Y. Fundamental Study on the Effect of Pulp Viscosity on Gangue Entrainment in Chalcopyrite Flotation. Master's Thesis, China University of Mining and Technology, Xuzhou, China, 2021.
37. Wang, C.; Sun, C.; Liu, Q. Entrainment of Gangue Minerals in Froth Flotation: Mechanisms, Models, Controlling Factors, and Abatement Techniques—A Review. *Min. Reclam. Environ.* **2021**, *38*, 673–692. [[CrossRef](#)]

Disclaimer/Publisher's Note: The statements, opinions and data contained in all publications are solely those of the individual author(s) and contributor(s) and not of MDPI and/or the editor(s). MDPI and/or the editor(s) disclaim responsibility for any injury to people or property resulting from any ideas, methods, instructions or products referred to in the content.